Supporting Information

Anion(I^-)-π(bisphosphonium)$^{2+}$ Photoluminescence Enhanced by $[Pt(CN)_2(Me\text{-}phpy)]^-$

Dorota Glosz[1,2], Guillaume Calvez[3], Toni Eskelinen[4,5], Andrey Belyaev[6], Christophe Lescop[3], Igor O. Koshevoy[6]*, Robert Podgajny[1]*

[1] *Faculty of Chemistry, Jagiellonian University, Gronostajowa 2, 30-387 Krakow, Poland*

[2] *Doctoral School of Exact and Natural Sciences, Jagiellonian University, Lojasiewicza 11, 30-348 Krakow, Poland*

[3] *INSA Rennes, CNRS, ISCR (Institut des Sciences Chimiques de Rennes), UMR 6226, F-35000, Rennes, France*

[4] *Department of Chemistry and Materials Science, Aalto University, 00076 Aalto, Finland*

[5] *Institute for Chemical Research, Kyoto University, Uji, Kyoto 611-0011, Japan*

[5] *Department of Chemistry and Sustainable Technology, University of Eastern Finland, Yliopistokatu 7, 80101 Joensuu, Finland*

emails: igor.koshevoy@uef.fi (I. O. K.) robert.podgajny@uj.edu.pl (R. P.)

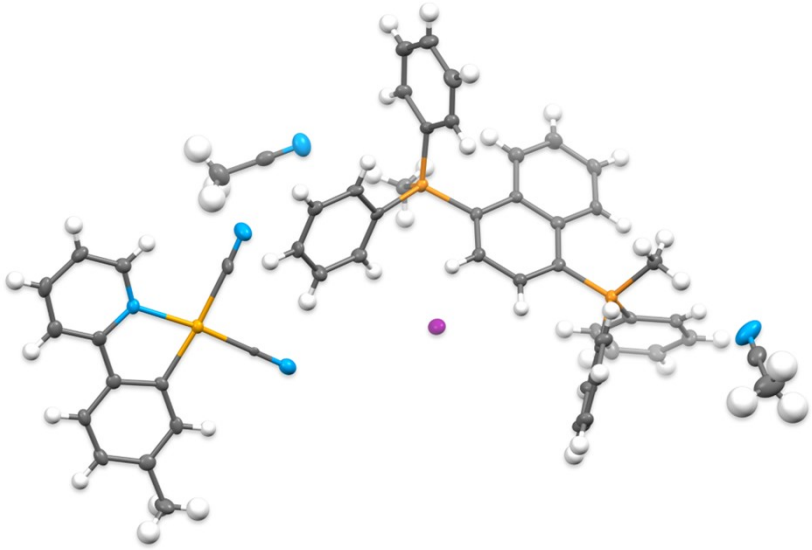

Figure S1. Asymmetric unit of **1**. Colors: C – gray, H – white, N – blue, P – orange, Pt – dark yellow, I – purple. Thermal ellipsoids are drawn at the 50% probability level.

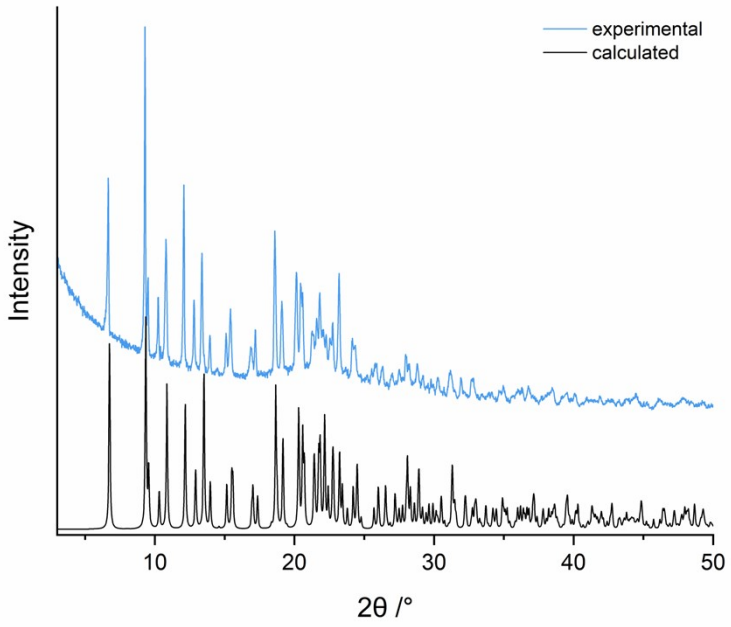

Figure S2. pXRD patterns for **1**: experimental (298 K; dry, ground crystals) and calculated from single crystal X-ray model (100 K).

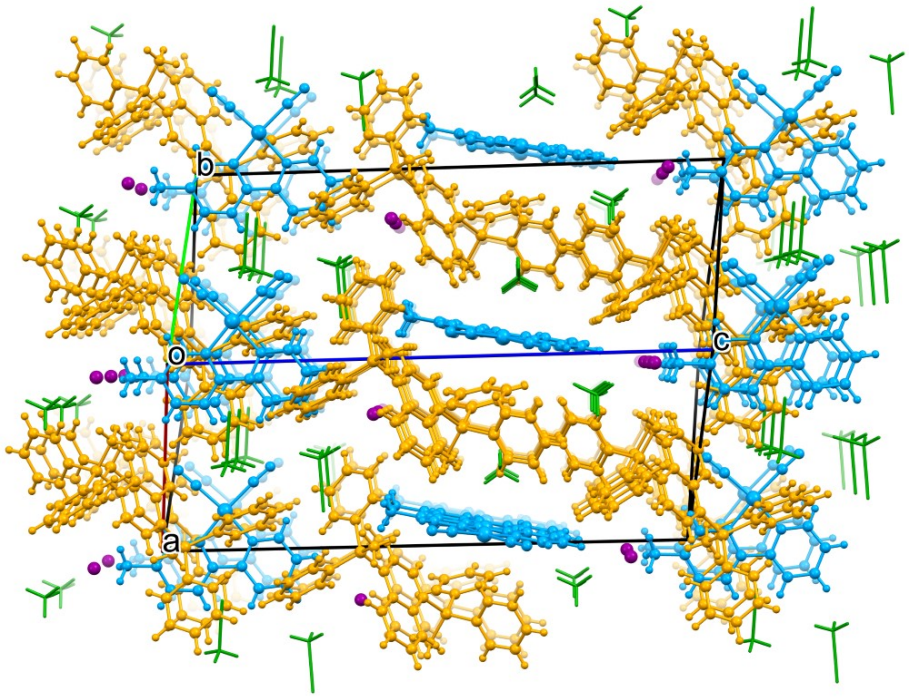

Figure S3. A fragment of crystal structure of **1** projected along the direction [110]. Color code: Pt complex – blue; dication – sand yellow; iodide anion – purple; MeCN – green.

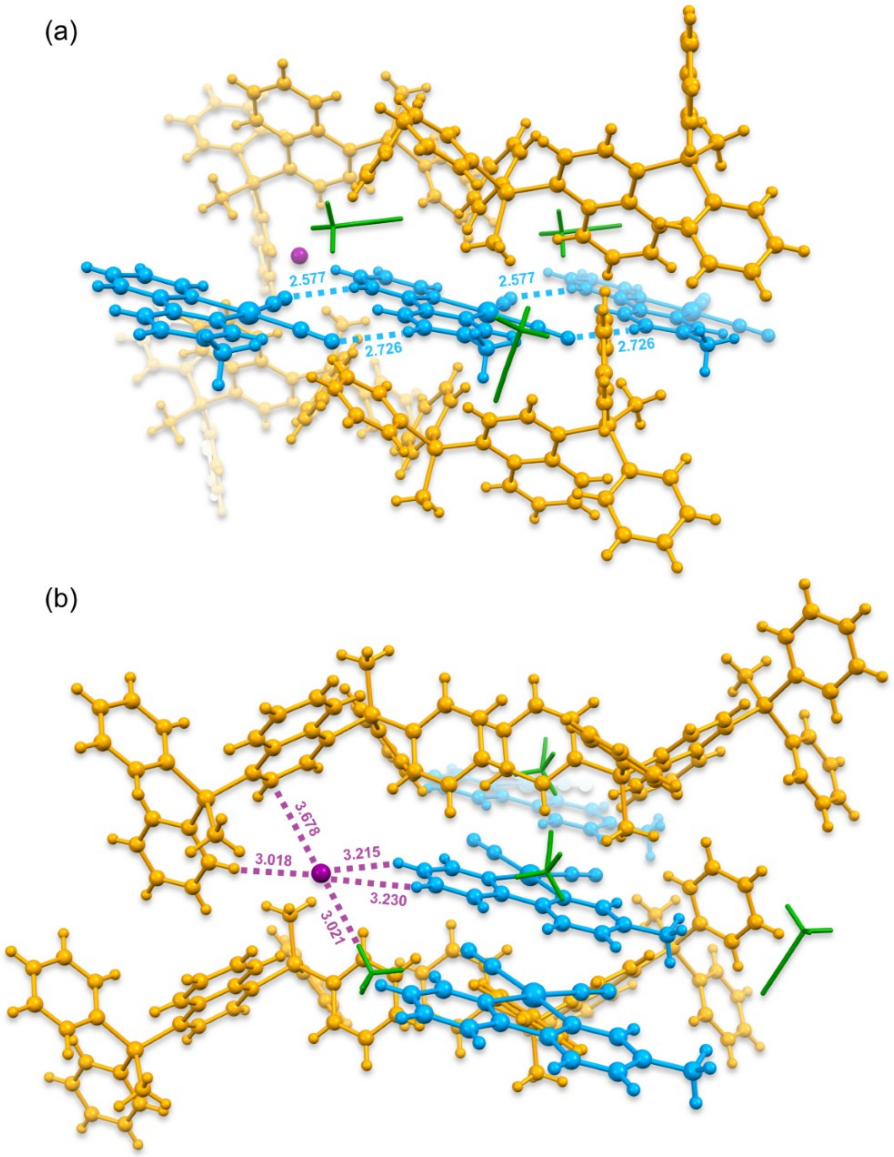

Figure S4. The portion of crystal structure of **1** showing the belt like Pt complexes arrangement. Upper section (**a**) is focused on $_{phpy}$C-H···N$_{cyano}$ contacts between complexes (blue dashed line; values in Å), whereas the bottom section (**b**) shows the closest contacts of iodide anions (purple dashed line; values in Å). Color code: Pt complex – blue; dication – sand yellow; iodide anion – purple; MeCN – green.

Acetonitrile molecules play secondary role in construction and stabilization of anion-π packing structure of **1**. The surroundings of iodide anions composed of the naphthyl ring and various C–H groups incorporates also weak $_{MeCN}$C–H···I$^-$ contacts (**b**). The nitrogen ends of MeCN tend to reside near the phosphorus centers of the cations contributing to overall packing.

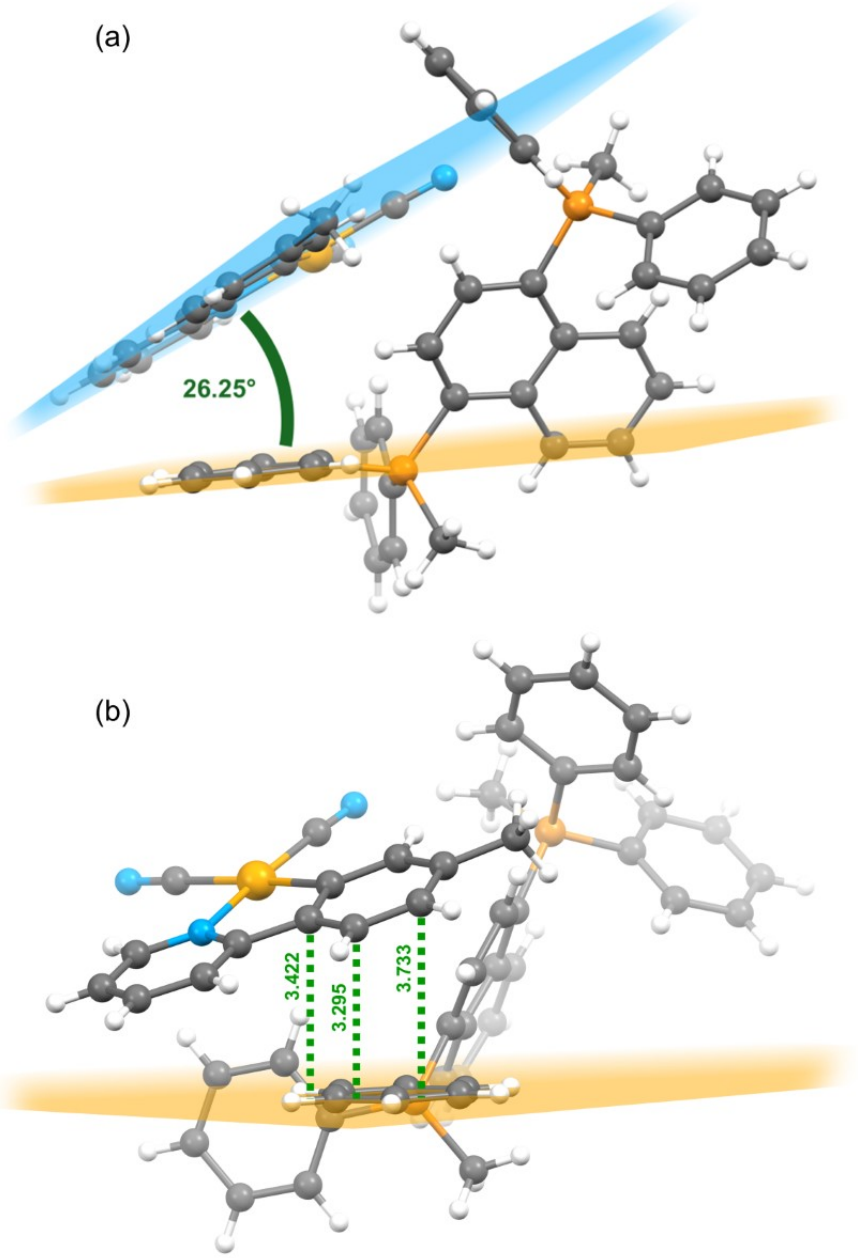

Figure S5. The angle between the phenyl ring of dication and chelate ligand of Pt(II) (**a**) together with the distances illustrative for the relevant π–π contacts (in Å) (**b**). The contacts indicated in (**b**) are defined as the distances between carbon atoms of the chelating ligand in Pt(II) complex and the plane established by the closest aromatic ring of dication. Colors: C – gray, H – white, N – blue, P – orange, Pt – dark yellow, I – purple.

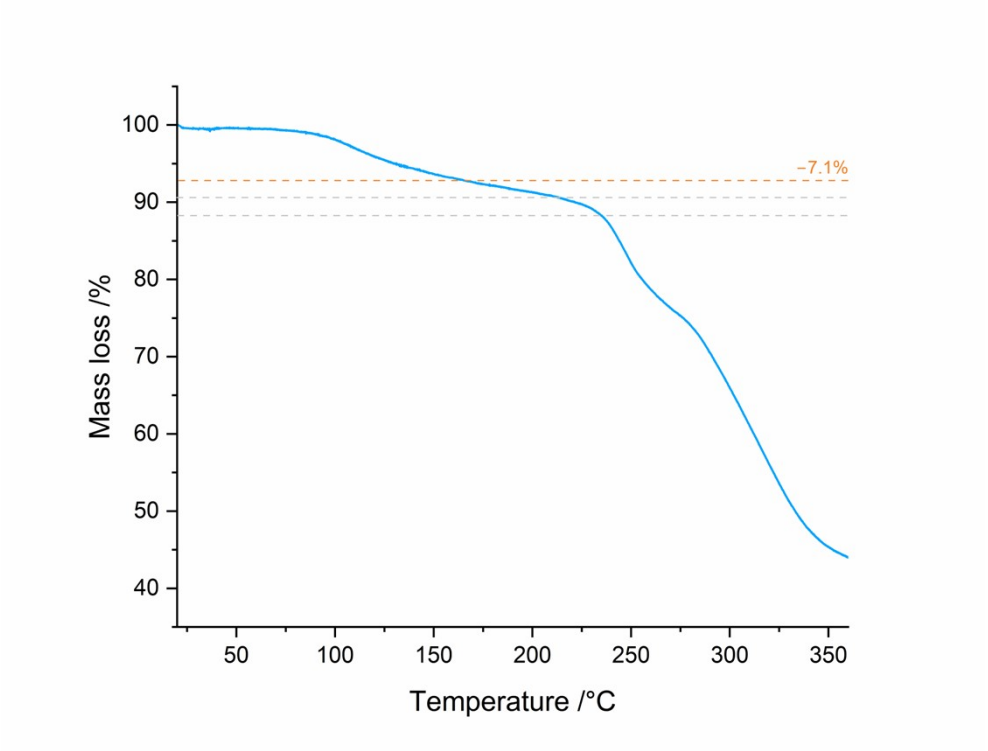

Figure S6. Thermogravimetric analysis for **1**. The observed mass loss starting around 80°C is attributable to the loss of crystallization acetonitrile molecules and, most probably, to a further loss of cyanido-ligands (calculations below), which leads to massive thermal decomposition above 230°C.

Formula	**Molar mass**
[1,4-nap($PMePh_2$)$_2$][Pt(CN)$_2$(Me-phpy)][I]·2MeCN (**1**)	1150.92 g/mol
[1,4-nap($PMePh_2$)$_2$][Pt(CN)$_2$(Me-phpy)][I]	1068.82 g/mol
difference: 82.1 g/mol; **7.1%** (between ca. 80 and ca. 180 °C)	
[1,4-nap($PMePh_2$)$_2$][Pt(CN)$_2$(Me-phpy)][I] – 1CN^-	1042.82 g/mol
difference: 108.3 g/mol; 9.4%	
[1,4-nap($PMePh_2$)$_2$][Pt(CN)$_2$(Me-phpy)][I] – 2CN^-	1016.80 g/mol
difference: 134.5 g/mol; 11.7%	

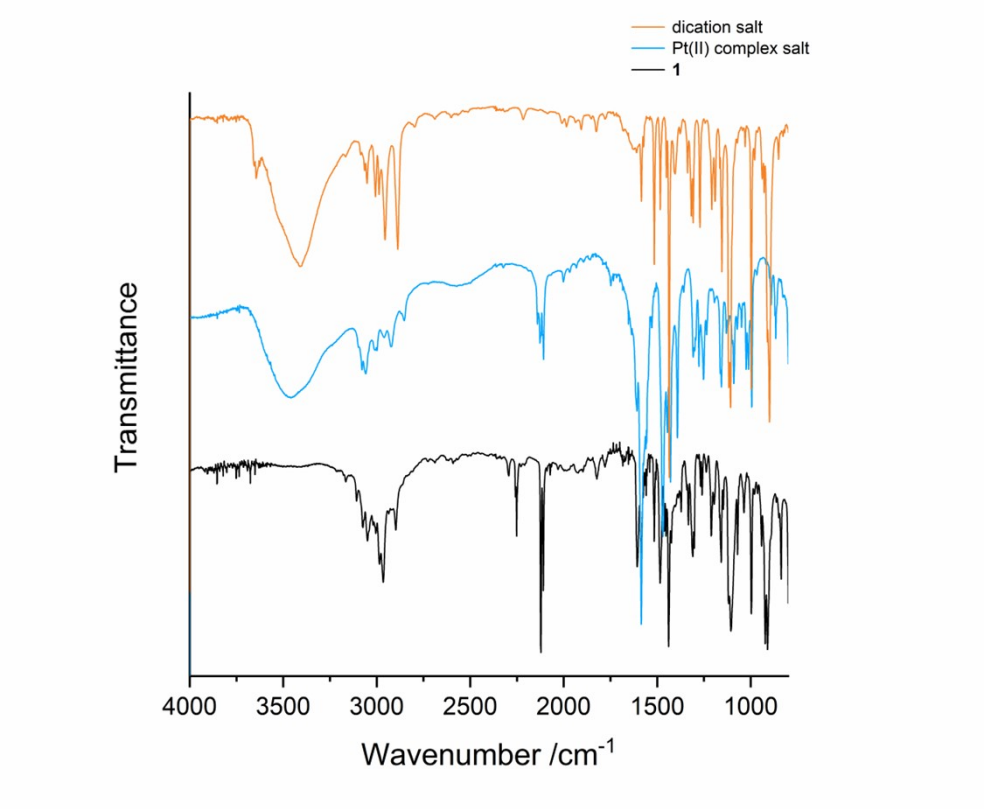

Figure S7. Solid state IR spectra of **1** compared with dication salt ([1,4-nap(PMePh$_2$)$_2$][I]$_2$) and Pt(II) complex potassium salt (K[Pt(CN)$_2$(Me-phpy)]). All structural components of **1** are represented in the spectrum: stretching *v*(C–H) vibrations of phenyl rings and MeCN and in the range 3200-2800 cm^{-1}, stretching *v*(C≡N) vibrations of crystallization MeCN at 2250 cm^{-1} and of Pt(II) complex in the 2135-2100 cm^{-1} range, and skeletal C–C and C–N vibrations of dication, Pt(II) complex salt, and MeCN in the fingerprint region.

Table S1. Crystal data and structure refinement of **1**.

Identification code	**1**
Empirical formula	$C_{54}H_{48}IN_5P_2Pt$
Formula weight	1150.90
Temperature	100.00 K
Wavelength	0.71073 Å
Crystal system	monoclinic
Space group	*Cc*
Unit cell dimensions	*a* = 13.9278(11) Å *b* = 13.0752(10) Å *c* = 26.608(2) Å
Unit cell angles	*α* = 90° *β* = 99.948(3)° *γ* = 90°
Volume	4772.7(6) $Å^3$
Z	4
Density (calculated)	1.602 g/cm^3
Absorption coefficient	3.696 mm^{-1}
F(000)	2272
Crystal size	0.10 x 0.09 x 0.03 mm
Theta range for data collection	2.199 to 25.027°
Index ranges	-16<=h<=16 -15<=k<=15 -31<=l<=31
Reflections collected	39746
Independent reflections	8001 [R(int) = 0.0448]
Completeness	99.6 %
Absorption correction	multi-scan
Max. and min. transmission	0.7454 and 0.6647
Data/restraints/parameters	8001/2/574
Goodness-of-fit on F^2	1.074
Final R indices [I>2sigma(I)]	R1 = 0.0228, wR2 = 0.0508
R indices (all data)	R1 = 0.0232, wR2 = 0.0510
Largest diff. peak and hole	0.952 and -0.354 $eÅ^{-3}$

Table S2. Computed transition energies (E) and wavelengths (λ), oscillator strengths (f), and predicted character of excitation and phosphorescence together with the energy differences between the first three excited singlets and the emissive triplet state, $\Delta E(S_n–T_1)$ (n = 1, 2 or 3), and the relevant spin-orbit coupling matrix elements, $\xi(S_n.T_1)$.

	Pt(II) anion $[Pt(CN)_2(Me\text{-}phpy)]^-$	dication monoiodide $\{[1,4\text{-}nap(PMePh_2)_2][I]\}^+$	**1**
	Excitation $S_0 \rightarrow S_1$		
E /eV	3.73	2.94	3.24
λ /nm	333	421	383
f	0.0818	0.1129	0.0579
Character	MLCT/ILCT	iodide-π* CT	iodide-π* CT
	Phosphorescence $T_1 \rightarrow S_0$		
E /eV	2.38	1.78	1.83
λ /nm	521	696	678
f	0.0001	0.0002	0.0005
Character	MLCT/ILCT	iodide-π* CT	iodide-π* CT
$\Delta E(S_1–T_1)$[a] /eV	0.39	0.06	0.17
$\Delta E(S_2–T_1)$[b] /eV	1.36	0.64	0.92
$\Delta E(S_3–T_1)$[b] /eV	1.70	0.68	0.96
$\xi(S_1.T_1)$[c] /cm^{-1}	84	184	305
$\xi(S_2.T_1)$[d] /cm^{-1}	1097	1888	1758
$\xi(S_3.T_1)$[d] /cm^{-1}	608	1834	1723

[a] vertical energy difference at S_1 geometry; [b] vertical energy difference at T_1 geometry; [c] at S_1 geometry; [d] at T_1 geometry.

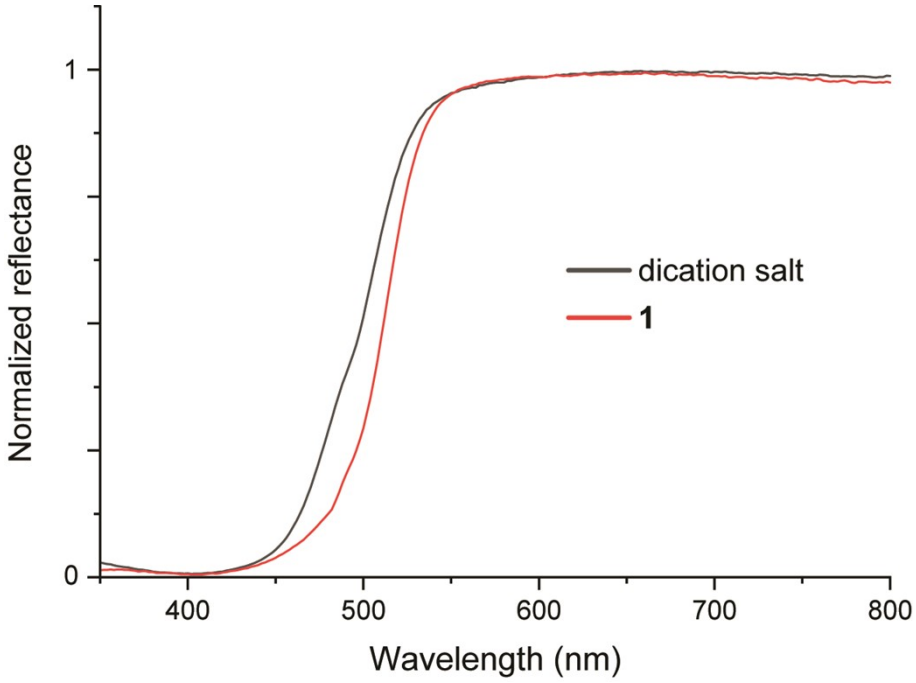

Figure S8. Diffuse reflectance spectra of dication salt ($[1,4\text{-nap}(PMePh_2)_2][I]_2$) and **1** at 298 K.

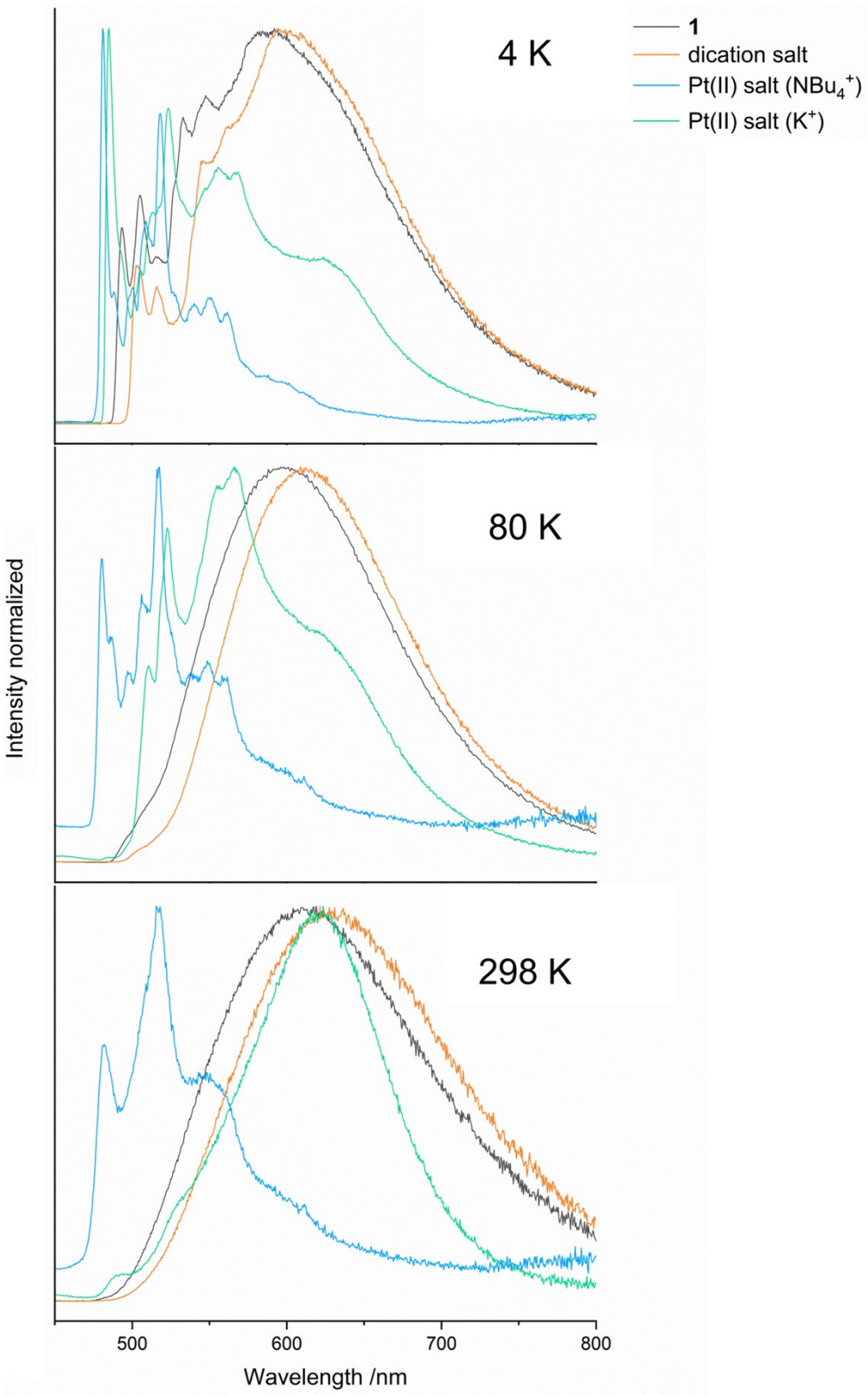

Figure S9. Normalized solid-state emission spectra of **1**, dication salt ([1,4-nap($PMePh_2$)$_2$][I]$_2$), and Pt(II) salts (NBu_4[Pt(CN)$_2$(Me-phpy)] and K[Pt(CN)$_2$(Me-phpy)]) at 4 K, 80 K, and 298 K (λ_{exc} = 325 nm).

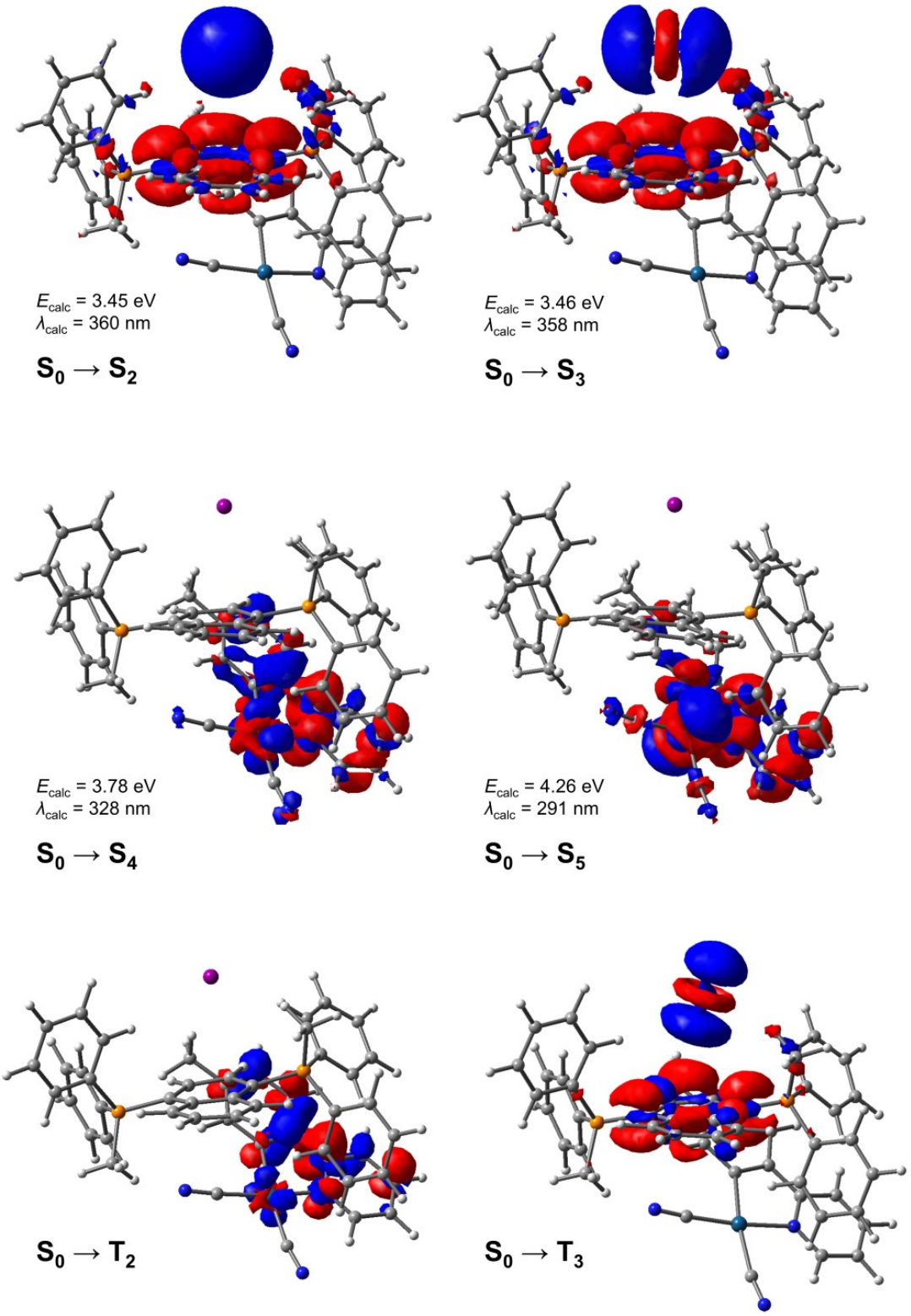

Figure S10. Higher energy excitations ($S_0 \rightarrow S_2$, $S_0 \rightarrow S_3$, $S_0 \rightarrow S_4$, $S_0 \rightarrow S_5$, $S_0 \rightarrow T_2$, $S_0 \rightarrow T_3$) electron density difference plots for salt **1,** together with calculated corresponding transition wavelengths (λ_{calc}) and energies (E_{calc}). During the electronic transition, the electron density decreases in the blue areas and increases in the red areas.

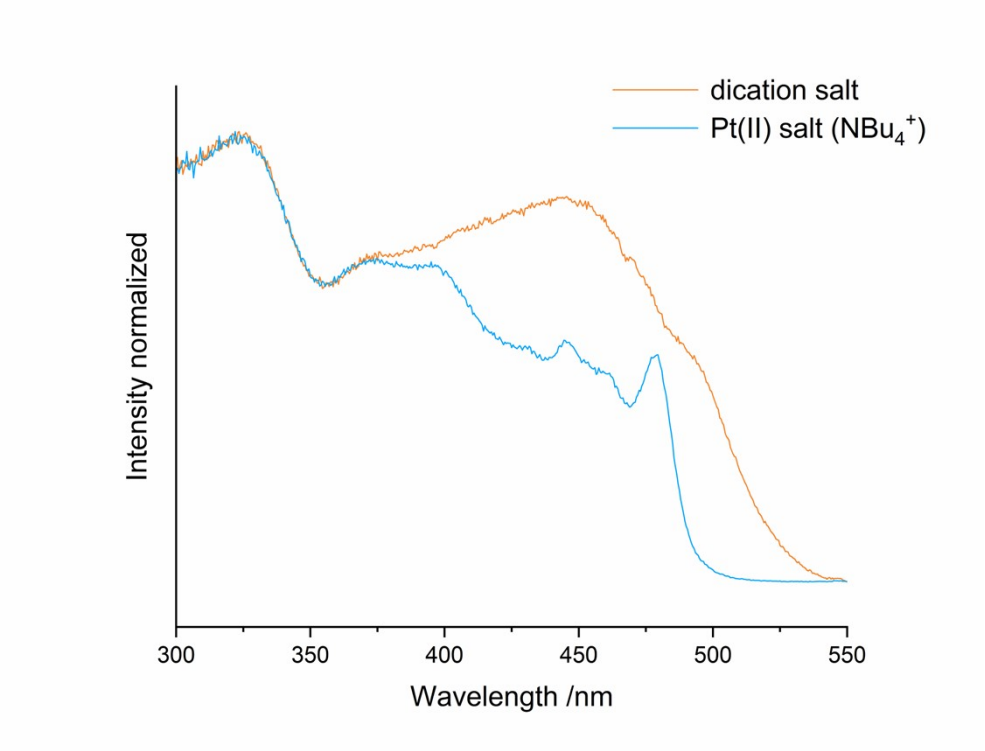

Figure S11. Excitation spectra of Pt(II) salt ($NBu_4[Pt(CN)_2(Me\text{-}phpy)]$) and dication salt ($[1,4\text{-}nap(PMePh_2)_2][I]_2$) at 298 K ($\lambda_{em}$ = 600 nm).

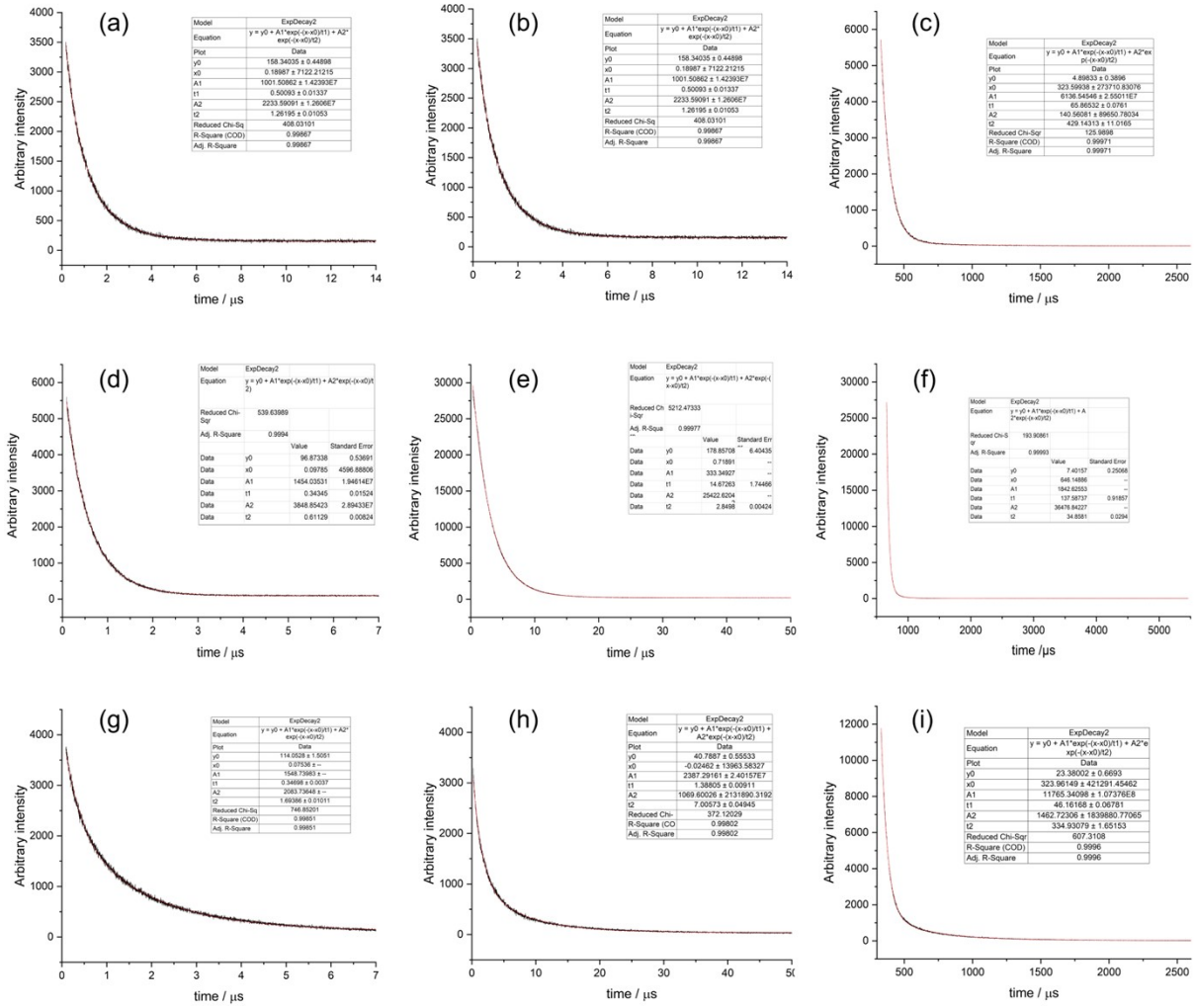

Figure S12. Profiles of the decays of the luminescence signal measured for solid samples of **1**: 298 K (**a**), 80 K (**b**), 4 K (**c**), [1,4-nap(PMePh$_2$)$_2$][I]$_2$: 298 K (**d**), 80 K (**e**), 4 K (**f**), K[Pt(CN)$_2$(Me-phpy)]: 298 K (**g**), 80 K (**h**), 4 K (**i**).